Start Sites of Bidirectional DNA Synthesis at the Human Lamin B2 Origin

Gulnara Abdurashidova,[1]* Marta Deganuto,[1]* Raffaella Klima,[1] Silvano Riva,[2] Giuseppe Biamonti,[2] Mauro Giacca,[3] Arturo Falaschi[1]†

The initiation sites of bidirectional synthesis at the DNA replication origin located at the 3′ end of the human lamin B2 gene were investigated. RNA-primed nascent DNA molecules were subjected to second-strand synthesis with appropriate primers, amplified by ligation-mediated polymerase chain reaction, and size fractionated. Evidence for precise start sites was obtained. Exploration of close to 1 kilobase, coupled to inhibition of Okazaki fragment synthesis, demonstrates that the leading strands initiate at precise nucleotides on either helix, overlapping by three base pairs, within the area bound to a protein complex possibly analogous to the prereplicative complex of yeast.

Origins of DNA replication (ori) are the chromosomal regions from which bidirectional duplication of replicons initiates, as well as the elements on which, after specific protein-DNA interactions, regulation of the process occurs. Similar to what was previously observed in viral genomes (*1*), Bielinsky and Gerbi have been able to identify at the single nucleotide level the start sites of leading-strand synthesis in the *Saccharomyces cerevisiae* autonomously replicating sequence ARS1 ori (*2*), located inside the region interacting with replication-specific proteins (*3, 4*). It appears worthwhile to try and identify at the nucleotide level the transition points between continuous and discontinuous DNA synthesis at a metazoan ori; if these were found to reside within or near the replicative complexes, the contention would be reinforced that replication origins analogous to those described in eukaryotic microorganisms do indeed exist in metazoans. To this purpose, we have investigated the origin that in past years we had mapped on human chromosome 19, within 474 base pairs (bp) overlapping the 3′ end of the lamin B2 gene and the promoter of the *ppv1* gene (*5–7*). This origin shows, by in vivo footprinting analysis, a very prominent protection over a sequence partially overlapping the 3′ end of the lamin B2 gene (*8, 9*). The protection undergoes a cell-cycle–dependent modulation, in analogy with the larger and shorter footprints corresponding to the prereplicative and postreplicative complexes, respectively, of *S. cerevisiae* (*10*).

To detect the possible start sites of DNA synthesis at the lamin B2 ori we used as starting material nascent single-stranded DNA isolated from asynchronously growing cells, size fractionated by sucrose gradient (*7*), and treated with λ-exonuclease (an enzyme that is unable to degrade RNA-primed sequences and thus reduces contamination of the sample with randomly sheared DNA) (supplementary material is available at www.sciencemag.org/feature/data/1046041.shl, item 1). This population of DNA molecules contains a good representation of the newly replicated sequences at the origins firing shortly before the arrest of the culture [the lamin B2 ori is known to fire within 3 min of entry in S phase (*5*)]. In nascent DNA samples from yeast cells, the RNA-DNA junc-

[1]Molecular Biology and [3]Molecular Medicine Units, International Centre for Genetic Engineering and Biotechnology, Padriciano 99, 34012 Trieste, Italy. [2]Istituto di Genetica Biochimica ed Evoluzionistica of the Consiglio Nazionale delle Ricerche, Via Abbiategrasso 207, 27100 Pavia, Italy.

*These authors contributed equally to this work.
†To whom correspondence should be addressed. E-mail: falaschi@icgeb.trieste.it

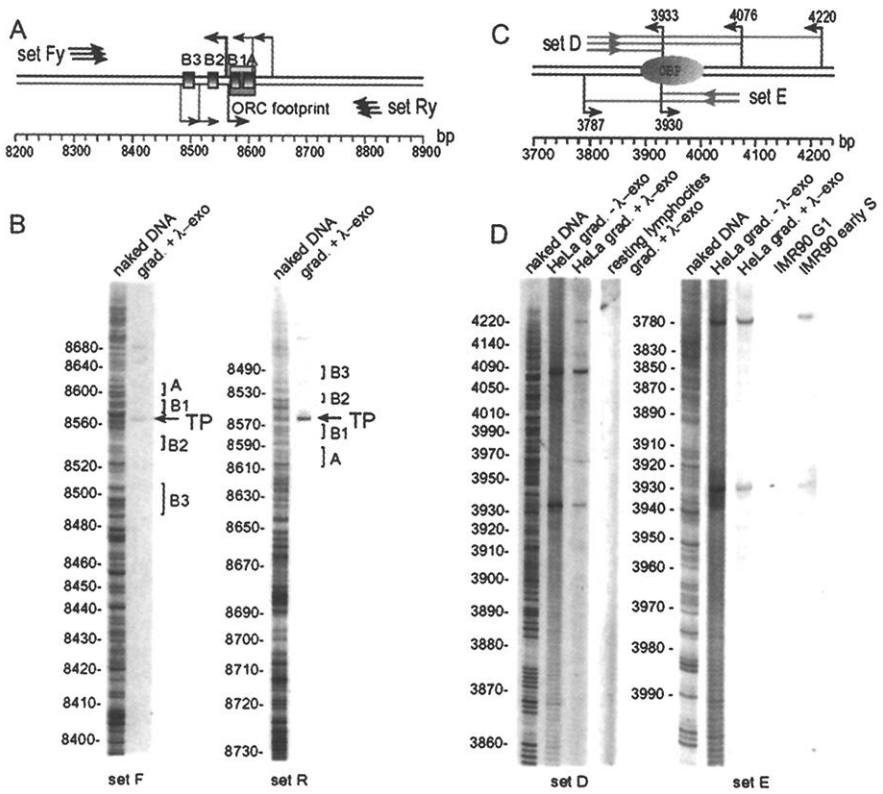

Fig. 1. Identification of precise start sites of nascent DNA synthesis within the protected area. **(A)** Yeast ARS1 region. Positions of sequence elements A, B1, B2, and B3 are marked by boxes. Localization and orientation of primer sets Fy and Ry used for LM-PCR are shown. **(B)** LM-PCR analysis of 0.01 μg of total genomic DNA or of about 10^4 molecules of size-fractionated, λ-exonuclease–digested nascent DNA isolated from asynchronously growing yeast cells. Positions of the transition points (TP) from continuous to discontinuous DNA synthesis are shown to correspond to the published data (*1*). **(C)** Schematic representation of DNA-protein interactions (origin binding proteins; OBP) at the lamin B2 ori (*9*). Pale arrows indicate localization and orientation of the primer sets used. Thin lines connected to primers indicate the lengths of their relative extended products. Start sites of nascent DNA synthesis are shown by black arrows. Numbers correspond to those of the file humlambbb of GenBank (accession number M94363). **(D)** LM-PCR analysis of in vitro dimethyl sulfate-treated genomic DNA (2 μg), size-fractionated DNA isolated from asynchronously growing cells (about 10^4 molecules), and total DNA isolated from cells synchronized at the indicated phase of the cell cycle (about 10^4 molecules). Where indicated, samples were treated with λ-exonuclease.

tions resulting from the DNA replication process have been successfully identified by complementary strand synthesis with appropriate primers (*2*). Primer extension, however, is not sufficiently sensitive in view of the size of the human genome. Therefore, we took advantage of a ligation-mediated polymerase chain reaction (LM-PCR) procedure for amplification of the detected DNA segments (*11*) (supplementary material is available at www.sciencemag.org/feature/data/1046041.shl, item 2).

To validate this approach, size-fractionated nascent DNA isolated from asynchronously growing yeast cells and treated with λ-exonuclease was analyzed by LM-PCR (supplementary material is available at www.sciencemag.org/feature/data/1046041.shl, items 2 and 3) by using two sets of primers located on either side of the ARS1 ori (Fig. 1, A and B). As shown in Fig. 1B, we identified exactly the same start sites of leading-strand synthesis as previously detected (*2*), but we used an amount of nascent DNA that was lower by five orders of magnitude.

We began our search for the possible start sites at the lamin B2 ori with primer sets D and E (Fig. 1, C and D) firing from either side of the protected region toward each other. With primer set D, even without λ-exonuclease treatment, discrete stop sites of second-strand synthesis (and hence of RNA-DNA junction) are visible—the first at nucleotide 3933, the second at nucleotide 4076, and the third at a less precise position; these data are much more evident after λ-exonuclease treatment. The analysis with primer set E gives specular results: two clear sites of RNA-DNA junction are visible, one at nucleotide 3930 and the other at nucleotide 3787. The same experiment on size-fractionated DNA from quiescent human lymphocytes gave no evidence of any stop site for primer set D. Furthermore, with DNA extracted from IMR-90 cells synchronized in G_1 phase and at the beginning of S, analyzed with primer set E, no stop sites are visible in G_1 cells, whereas those that have just entered S show precise stop sites in exactly the same positions as the asynchronously growing cells.

Thus, nucleotides 3933 and 3930, located within the protected area, might correspond to the starts of the leading strands moving leftward and rightward, respectively, whereas the RNA-DNA junctions observed about 140 nucleotides upstream of both could derive from ligation of the first Okazaki fragment to the respective leading-strand start. Would primers displaced at different distances on either side of the proposed start sites give results consistent with this interpretation? To answer this question, we further analyzed upper nascent DNA strands with primer sets H, D, G, and B (see Fig. 2, A and B). If we move 50 nucleotides closer than primer set D to the putative start site of bidirectional DNA replication with primer set H, we obtain the results shown in Fig. 2B, which indicate again nucleotide 3933 as the likely start site of a leading strand and nucleotide 4076 as the possible start of the first lagging-strand fragment (in perfect agreement with the result obtained in parallel with primer set D) plus a third stop around nucleotide 4200.

If, by using primer set G, we now move over 300 nucleotides in the 5′ direction from nucleotide 3933, hence at a distance greater than the length of an Okazaki fragment, we see only one single stop site at a position compatible with nucleotide 3933. The long blank region before this fragment indicates that we are dealing with continuous DNA synthesis and points to nucleotide 3933 as the transition point between continuous and discontinuous DNA replication. Thus, the data obtained with primer sets D, G, and H indicate nucleotide 3933 as the start site for the leftward leading strand.

This tentative conclusion is confirmed with primer set B, located approximately 200 nucleotides to the right of nucleotide 3933; several stop sites are visible at the indicated positions. These data can be interpreted as deriving from the linking to the initiated ori of four subsequent Okazaki fragments having lengths of 143, 144, 65, and 80 nucleotides from the first to the fourth, respectively; the results are also compatible with the presence of multiple alternative start sites of leading-strand synthesis. It is noteworthy that, when we performed the analysis with primer set B on DNA extracted from cells synchronized in G_1, at the beginning of S, and in mitosis, we confirmed that only the cells that have just initiated DNA synthesis show the presence of fragments of the already observed sizes.

We analyzed lower nascent DNA strands with primer sets C, A (displaced to the right of nucleotide 3930), and F (displaced to its left) (Fig. 2, A and C). With primer set C we obtained again a clear indication that the first stop site corresponds to nucleotide 3930, and a second one is at a length compatible with nucleotide 3787, in agreement with the data obtained with primer set E (see above and Fig. 1). With primer set A, we observed only one stop site at a very large size (compatible with its localization at nucleotide 3930); the long, >450-nucleotide region free of stop sites indicates that we are dealing with an area of continuous leading-strand synthesis and that nucleotide 3930 is the

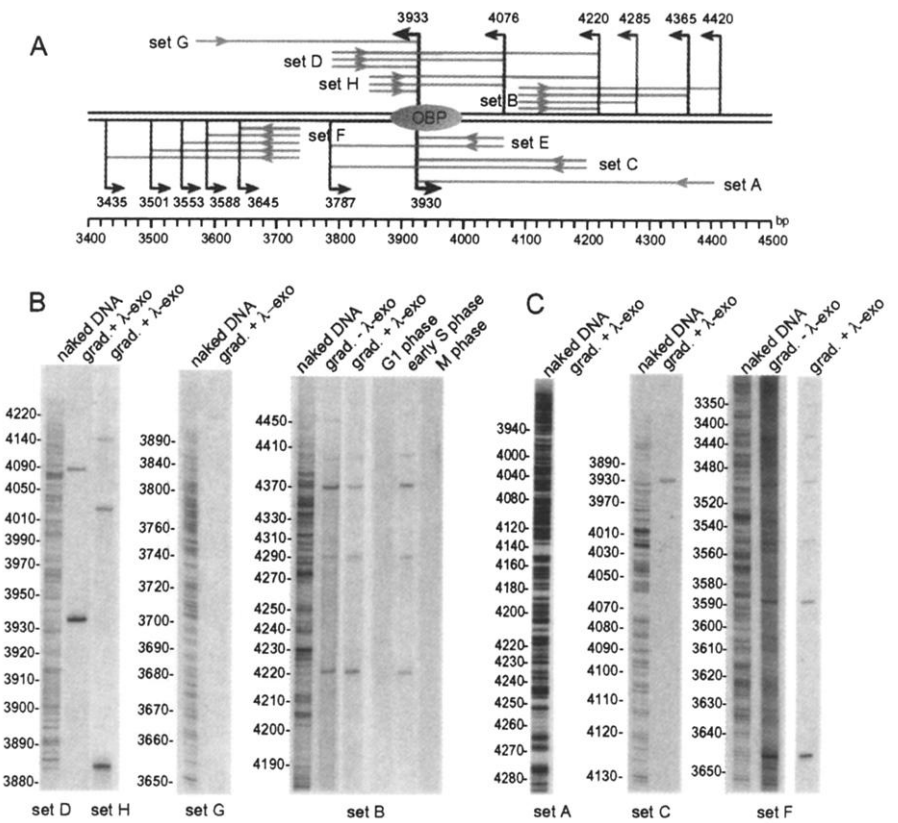

Fig. 2. Distribution of start sites of nascent DNA synthesis around the ori. (**A**) Localization and orientation of the primer sets in the analyzed 1-kb region. Position of the first detectable start site of leading-strand synthesis is indicated by thick arrows, and start sites of nascent DNA synthesis located more upstream are indicated by thinner arrows, all pointing in the direction of synthesis. (**B** and **C**) LM-PCR analysis on lower and upper strand, respectively, of size-fractionated newly replicated DNA from asynchronously growing HeLa cells or total DNA from synchronized IMR-90 cells subjected or not subjected to λ-exonuclease treatment as indicated. Amount of DNA and symbols are as in Fig. 1.

start site of the rightward moving leading strand. Conversely, with primer set F a number of start sites can be located precisely at the indicated positions, possibly corresponding to ligation of the first Okazaki fragments, having lengths (in the order of fork movement) of 143, 142, 67, 35, and 52, plus two more of about 65 nucleotides.

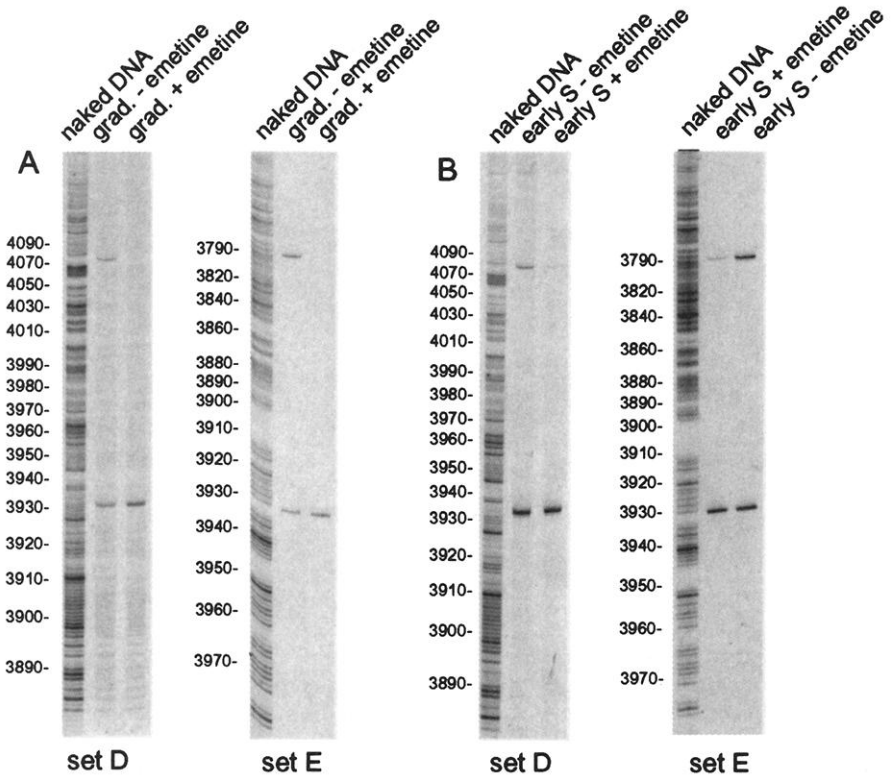

Fig. 3. Lamin B2 ori has a single start site of leading-strand synthesis. LM-PCR analysis of size-fractionated, λ-exonuclease-treated nascent DNA isolated from asynchronous cells (**A**) or from cells synchronized at the beginning of S phase (**B**) grown for 1 hour in the presence or absence of 2 μM emetine.

Thus, our analysis spanning a region of almost 1 kb identifies nucleotides 3933 and 3930 (within the protected area of the ori region) as the transition points between continuous and discontinuous DNA synthesis for upper and lower nascent DNA, respectively, but the possibility that the other stop sites of second-strand synthesis could arise from a multiplicity of start sites of leading-strand synthesis cannot be ruled out. We investigated this alternative interpretation (see Fig. 3) by isolating nascent DNA from HeLa cells incubated with emetine for 1 hour [a treatment that inhibits synthesis of Okazaki fragments (*12*)] and probing it with primer sets D and E. For both primers the emetine treatment does not affect the intensity of the signals at the positions corresponding to the starts of the leading strands, whereas it causes a fading down to disappearance of the signals interpreted as Okazaki fragment starts. Furthermore, when total DNA extracted from HeLa cells synchronized at the G_1/S border (supplementary material is available at www.sciencemag.org/feature/data/1046041.shl, item 1) and then released in S phase for 1 hour in the presence of emetine was analyzed by the same procedure, the signals of the start sites of the leading strands were not affected, whereas those corresponding to the starts of Okazaki fragments were significantly reduced on both sides of the ori.

Figure 4 summarizes our results and also reports the detailed protein-DNA interactions occurring in the ori area during the cell cycle. In agreement with what was reported for replicons studied at comparable detail (*1, 2*), synthesis of the oppositely moving leading strands starts

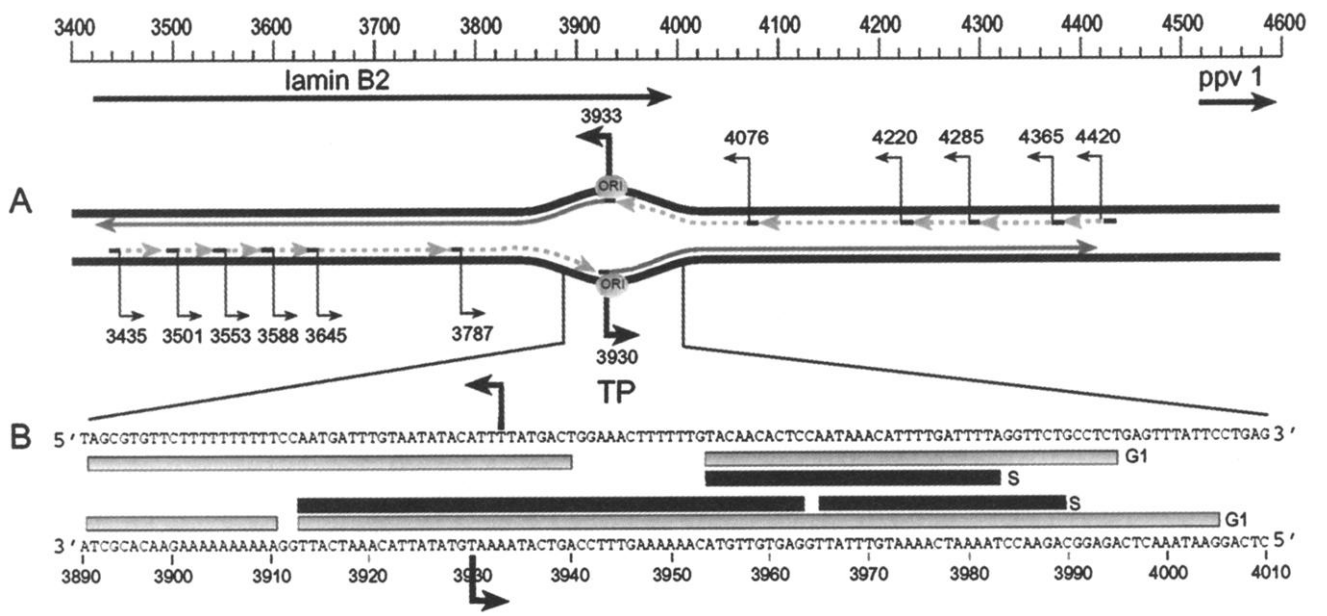

Fig. 4. Map of start sites of bidirectional DNA synthesis at the human lamin B2 ori. (**A**) Transition points (TP) from continuous to discontinuous DNA synthesis on the two strands are shown by thick arrows; 5′ ends of Okazaki fragments are indicated by thin arrows. Positions of the transcripts around ori area are shown. (**B**) Precise positions of the protein-DNA interactions occurring in G_1 and S phase (*9*) are shown by gray and black boxes, respectively.

almost at the same positions on the two complementary helices: in the yeast ARS1 origin, the start sites of the two leading strands are displaced by 2 bp (*1*) and in the human lamin B2 origin they overlap by 3 bp. As in yeast, the initiation event occurs within an A+T-rich area where specific nucleoprotein complexes assemble in G_1 and S phase. In both systems initiation occurs within the extended protected region detectable in G_1. From our data it is also apparent that, on the retrograde arms, in both directions, the first two Okazaki fragments are of nearly identical length, close to 140 nucleotides, whereas the following ones (up to the fifth or sixth) are shorter.

We are currently addressing identification of the proteins belonging to these complexes and we intend to check the possibility that some of them might be the human counterparts of the yeast ORC and MCM proteins (*13*).

References

1. R. T. Hay and M. L. DePamphilis, *Cell* **28**, 767 (1982); H. H. Niller, G. Glaser, R. Knuchel, H. Wolf, *J. Biol. Chem.* **270**, 12864 (1995).
2. A. K. Bielinsky and S. A. Gerbi, *Science* **279**, 95 (1998); *Mol. Cell* **3**, 477 (1999).
3. Y. Marahrens and B. Stillman, *EMBO J.* **13**, 3395 (1994).
4. A. D. Donaldson and J. J. Blow, *Curr. Opin. Genet. Dev.* **9**, 62 (1999).
5. G. Biamonti *et al.*, *Chromosoma* **102**, S24 (1992).
6. M. Giacca *et al.*, *Proc. Natl. Acad. Sci. U.S.A.* **91**, 7119 (1994); M. Giacca, C. Pelizon, A. Falaschi, *Methods* **13**, 301 (1997).
7. S. Kumar *et al.*, *Nucleic Acids Res.* **24**, 3289 (1996).
8. D. Dimitrova *et al.*, *Proc. Natl. Acad. Sci. U.S.A.* **93**, 1498 (1996).
9. G. Abdurashidova, S. Riva, G. Biamonti, M. Giacca, A. Falaschi, *EMBO J.* **17**, 2961 (1998).
10. J. F. Diffley, J. H. Cocker, S. J. Dowell, A. Rowley, *Cell* **78**, 303 (1994).
11. J. P. Quivy and P. B. Becker, *Nucleic Acids Res.* **21**, 2779 (1993).
12. W. C. Burhans *et al.*, *EMBO J.* **10**, 4351 (1991).
13. K. A Gavin, M. Hidaka, B. Stillman, *Science* **270**, 1667 (1995); S. E. Kearsey and K. Labib, *Biochim. Biophys. Acta* **1398**, 113 (1998); D. G. Quintana *et al.*, *J. Biol. Chem.* **272**, 28247 (1997); D. G. Quintana *et al.*, *J. Biol. Chem.* 273, 27137 (1998); T. Tugal *et al.*, *J. Biol. Chem.* **273**, 32421 (1998).

6 October 1999; accepted 2 February 2000

A Role for Nuclear Inositol 1,4,5-Trisphosphate Kinase in Transcriptional Control

Audrey R. Odom,[1] Alke Stahlberg,[2] Susan R. Wente,[2] John D. York[1]*

Phospholipase C and two inositol polyphosphate (IP) kinases constitute a signaling pathway that regulates nuclear messenger RNA export through production of inositol hexakisphosphate (IP_6). The inositol 1,4,5-trisphosphate kinase of this pathway in *Saccharomyces cerevisiae*, designated Ipk2, was found to be identical to Arg82, a regulator of the transcriptional complex ArgR-Mcm1. Synthesis of inositol 1,4,5,6-tetrakisphosphate, but not IP_6, was required for gene regulation through ArgR-Mcm1. Thus, the phospholipase C pathway produces multiple IP messengers that modulate distinct nuclear processes. The results reveal a direct mechanism by which activation of IP signaling may control gene expression.

How diverse extracellular stimuli elicit selective cellular responses through the activation of IP signaling pathways remains an important question in eukaryotic biology. Central to this process is phosphatidylinositol-specific phospholipase C, activation of which produces second messenger molecules such as inositol 1,4,5-triphosphate (IP_3), a regulator of calcium release (*1, 2*). Modification of IP_3 to form higher phosphorylated inositols such as IP_4, IP_5, and IP_6, the functions of which are less well understood, indicates that the regulatory effects of IP messengers may not be limited to calcium signaling (*2, 3*). Further diversity may be achieved through the spatial localization of IP pathways to cellular organelles (*4*). For example, a phospholipase C–dependent IP kinase signaling pathway contributes to IP_6-mediated mRNA export from the nucleus. In this pathway, phosphatidylinositol 4,5-bisphosphate is hydrolyzed to IP_3, which is then sequentially phosphorylated to IP_6 by two IP kinases: a putative kinase with dual specificity for IP_3 and IP_4, whose locus has not been mapped, and an IP_5 2-kinase (Ipk1) that is localized to the nuclear envelope–pore complex (*5*).

Many agonists that activate IP signaling also initiate specific changes in gene expression. Tight control of transcription is facilitated through the assembly of site-specific protein complexes on DNA promoter elements that regulate the activity of the general transcriptional machinery. One such multiprotein assembly is the arginine-responsive ArgR-Mcm1 complex, which comprises four proteins—Arg80, Arg81, Arg82, and Mcm1—each of which is required for proper transcriptional control (*6, 7*). Arg80 and Arg81 function as arginine-specific transcription factors, whereas Arg82 and Mcm1 are pleiotropic regulators. Mutants of *arg82* have defects in responses to nutrients, sporulation, mating, and stress (*8*). Mcm1 is a versatile transcription factor required for regulation of diverse gene sets including those involved in cell-cycle control, cell-type specificity, and pheromone and nutrient responses (*6, 9*). As a canonical member of the MADS (*MCM1*, agamous, deficiens, serum response factor) box transcription factor family, Mcm1 typically acts in concert with factors that have more limited cellular roles to achieve specificity in transcriptional control (*10*). Thus, combinatorial interplay between the dedicated arginine-specific transcription factors Arg80 and Arg81 and the more general factors Mcm1 and Arg82 allows interpretation of changes in extracellular arginine levels into transcriptional control of genes that participate in biosynthesis and catabolism of arginine. We find that Arg82 is a dual-specificity IP_3-IP_4 kinase and thus establish a potential link between phospholipase C–activated IP signaling and transcriptional control.

The phospholipase C–dependent IP signaling pathway apparently uses a single gene product to convert IP_3 to IP_5. IP_3 and IP_4 kinase activities copurify from both budding and fission yeast extracts through multiple chromatography steps (*11*). Also, a mutation of a single locus in *Saccharomyces cerevisiae*, *GSL3*, results in the loss of IP_4 and IP_5 production in vivo (*5*). To identify the IP_3-IP_4 kinase, we speculated that an evolutionary relation might exist among IP_3 kinases. In metazoans, a family of IP_3 3-kinases has been identified (*12*). Multisequence alignment of this family was used to identify several conserved elements. These elements were then used to search the yeast database and revealed Arg82 as a candidate IP kinase with 30% identity and 55% similarity throughout two 30–amino acid conserved elements (Fig. 1). Arg82 has a predicted molecular mass similar to that of the purified yeast IP_3-IP_4 kinase activity (*11*).

To test directly whether *ARG82* encodes an intrinsic IP_3 kinase, we analyzed purified, recombinant Arg82. Incubation of recombinant protein with [^{3}H]inositol 1,4,5-trisphosphate and adenosine triphosphate (ATP) resulted in the formation of inositol 1,3,4,5,6-pentakisphosphate, indicating that Arg82 performs two phosphorylation steps (Fig. 2A). Recombinant Arg82 in the presence of pure inositol 1,4,5-

[1]Departments of Pharmacology and Cancer Biology and of Biochemistry, Duke University Medical Center, DUMC 3813, Durham, NC 27710, USA. [2]Department of Cell Biology and Physiology, Washington University School of Medicine, 660 South Euclid, St. Louis, MO 63110, USA.

*To whom correspondence should be addressed. E-mail: yorkj@acpub.duke.edu